Open Access Online Journal on Astronomy and Astrophysics

Acta Astrophysica Taurica

www.astrophysicatauricum.org

Acta Astrophys. Tau. 7(1), 8–11 (2026)

EDN: UTTPNS

TeA – Telescope Analyzer

E.V. Emelianov

Special Astrophysical Observatory of the Russian Academy of Sciences, Nizhnij Arkhyz 369167, Zelenchukskiy region, Karachai-Cherkessian Republic, Russia
e-mail: eddy@sao.ru

Received 15 December 2023

ABSTRACT

We have developed a multipurpose device for studying the optics and mechanics of the BTA and Zeiss-1000 telescopes. The heart of the device is a ZWO ASI 1600 MM Pro CMOS light detector mounted on a three-axis stage. The device was tested on the Zeiss-1000 and BTA telescopes. Based on the BTA tests, the spectrum of image oscillations along both axes was evaluated, as well as the possibility of using the device for estimating the aberration axis position (by direction of coma at the field of view), taking hartmannograms, and recording images of stellar fields to measure coefficients of the pointing correction system.

Key words: instrumentation, telescopes, optics control

1 Introduction

The idea of creating the Telescope Analyzer (TeA) has been under development for several years. Periodically, "technical" observations need to be carried out at the BTA and Zeiss-1000 telescopes to determine coefficients of the pointing correction system (PCS). While the standard Multi-Mode Photometer-Polarimeter (MMPP)[1] is used at Zeiss-1000 for this purpose, the Apogee CCD detector is used at the BTA, mounted either on its own flange (for operation in white light) or on a Shack – Hartmann sensor adapter (for operation in the narrow filter at 650 nm). After the failure of this detector, no instrumentation essentially remained that could be used to control the BTA PCS. During the alignment of the BTA primary mirror (PM) in 2018–2019, the problem of accurately determining the position of the mirror's aberration axis arose. The existing standard devices at the primary focus have an extremely small field of view, which doesn't allow accurate measurements based on coma orientation to be carried out. A detector with a sufficiently large field of view or the capability of being displaced to construct large-format mosaic frames was required.

The developed device has the following characteristics:

- Displacement range (relative to "zero limit switches"): $-30.75 \div 120$ mm along OX, $-20.5 \div 115$ mm along OY, $-18.5 \div 162.5$ mm along OZ. Near the flange: $-20.5 \div 70$ mm along OY.
- Center position: (48, 17) mm.
- Full field of view (relative to the geometric center): $-91.9 \div 76.5$ mm along OX, $-33.0 \div 70.9$ mm along OY (restricted range: $-33.0 \div 100.0$ mm).
- Maximum speeds (mm/s): $v_x = 7.5$, $v_y = 10$, $v_z = 15$.
- Positioning accuracy: ± 10 µm. Maximum flexure: 150 µm (span).

ZWO ASI 1600 MM Pro detector:

- 4/3″ (17.7×13.4 mm) – 150″×115″ at the BTA; 4656×3520 pixels (3.8 µm) – 0.033″/pixel.
- Capacity/readout noise/QE 20000 $\overline{e}$/1.2 $\overline{e}$/60 %. Dark (−20°C) 0.0062 $\overline{e}$/s/pixel.

2 Design

Figure 1 shows the device during its initial efficiency rating under laboratory conditions. In addition to the three-axis stage that moves the detector, there is a stand on the flange on which an industrial-grade mini-computer (the "heart" of the device control system), power supply units, and a control module for three stepper motors are mounted. The universal flange of the device allows it to be mounted directly, without any intermediate components, at the BTA primary focus or at the Cassegrain focus of Zeiss-1000.

During the initial development of the stepper motor control system, feedback via rotary encoders (1024 grooves per revolution) was not implied. However, it was found that that even at low speeds, the large mass of the device's nodes causes stepper motors to skip steps. This leads to a cumulative positioning error that can amount to millimeters over an entire observing night. To ensure accurate position measurements, linear encoders providing an accuracy of no worse

[1] https://www.sao.ru/Doc-k8/Telescopes/small/MMPP/

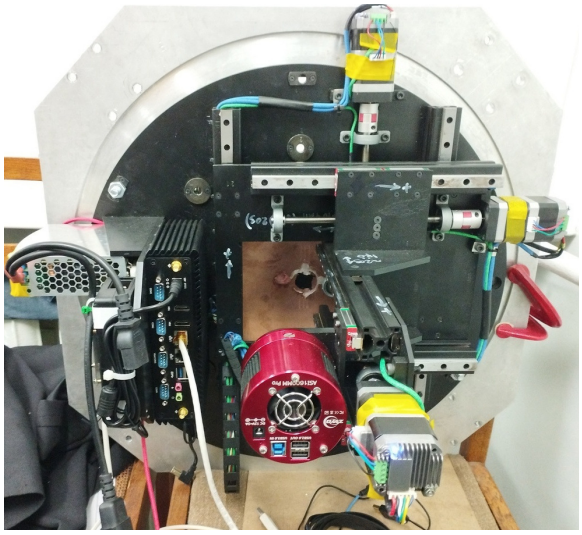

Fig. 1. External view of TeA.

than 10 ÷ 20 µm need to be mounted on each axis, which would significantly increase the cost of the device. Therefore, we decided to limit ourselves to measuring the precise position of the motor shafts using rotary optical encoders. With a thread of the screw pair of 1 mm, the encoder provides a discrete measurement of approximately 1 µm, which is sufficient to achieve the required positioning measurement accuracy of 1 motor step (200 steps per revolution, i.e., 5 µm per step).

After positioning is completed, power to the motors is removed; however, the microcontroller control module continues to monitor the shaft position and, in case of displacement, returns it to the initial position by moving the motor. Thus, the resulting closed-loop system allows a servo drive to be implemented.

3 Control system

3.1 Servo drives

The motor control system[2] was developed based on an STM32F072 microcontroller (MCU) with a Cortex-M0 core, which has a sufficient number of timers to acquire data from three encoders (quadrature output) and generate microstepping pulses for the stepper motor drivers (a step/dir driver with a 32 microstep division, placed directly on the motor housing). The encoders are mounted on the motor housings, and the optical disks are installed on the rear shaft (motors with a double-sided shaft are used). Connection to the host computer can be implemented through either USB or CAN interfaces (an option for integrating the controller into a network with other devices). Smooth start-up and deceleration of the motors is ensured by a trapezoidal ramp. Since power is removed from the motors after they come to a stop, intermediate positions (corresponding to fractional steps) are unavailable. Buttons for controlling stages are mounted on the controller housing (three buttons drive the corresponding axis to a conventional "positive" direction, another button reverses the direction along all axes, and an additional button allows the MCU to be reset if necessary).

When connected via USB, a text-based protocol is used. The controller emulates a popular PL2303 USB-UART converter, which allows it to be connected even to devices running Android. The text-based protocol enables control both from special software and directly from a terminal. If a command is entered incorrectly, the full list of available commands is displayed to the user, each of which must be terminated by a newline character (`'\n'`). A command without parameters is treated as a getter. If it is followed by a `'='` character, the command is treated as a setter. All settings are stored in the MCU's flash memory in EEPROM emulation mode (entries are written sequentially; the most recent entry is identified at the moment of switching on via binary search; when the configuration storage area runs out, it is fully erased and writing resumes from the beginning).

The command set can be divided into four conventional classes:

- Service commands (USB only): setting the CAN device identifier and network speed, entering the MCU firmware update mode, erasing saved settings, activating the CAN–USB bridge mode, etc.
- Motor control commands: moving to an absolute/relative position, stopping a running motor (both normal stop – through the ramp – and emergency stop), identifying the current motor position, and the current state of limit switches and motors.
- Editing and saving the configuration: ramp parameters (accelerations and maximum speeds) and encoder settings, the number of microsteps, the response to limit switches, etc.
- Other commands: current state of control buttons, signal levels at the analog-to-digital converter (ADC) inputs, enabling/disabling the audio signal, relay and pulse-width modulation (PWM) load control, changing the signals on external GPIO outputs, and others.

The packet format for operation on the CAN bus utilizes all eight available bytes. The MCU responds only to commands sent with the identifier specified in its configuration. Data are transmitted in little-endian format. The first two bytes contain the command code, the third byte is the command parameter (e.g., the motor or ADC channel number), the fourth byte is the error code (transmitted only in the response), and the last four bytes carry the command data in 32-bit signed integer format. The MCU's response is sent with the same identifier as the received commands. In a simplified format (without a parameter and data), it is permissible to transmit only two bytes in the packet, which is just a command code.

3.2 Detector

Given the need to work with different types of detectors, the author had previously developed a control system with a claim to universality[3]. It has a base core that parses

[2] https://github.com/eddyem/stm32samples/tree/master/F0:F030,F042,F072/3steppersLB

[3] https://github.com/eddyem/CCD_Capture

command-line parameters and performs the necessary operations (including basic viewing of the acquired images in an OpenGL window, which is an option that arose from the need for real-time visual inspection of images during instrument alignment), while direct communication with the detector application programming interfaces (APIs) is handled through plug-in modules implemented as dynamic libraries. A corresponding module was written for operating with ZWO detectors.

The detector control system can operate both in standalone mode and in client-server mode. In the latter case, only local INET sockets (or faster UNIX sockets) are used for security. In the current version of the system, images are transmitted to the client through the socket in uncompressed form; therefore, to accelerate this procedure in the future, it is planned to store images in shared memory so as to provide the client with direct access to the image immediately after readout is complete. To view on a remote computer that does not support OpenGL forwarding (if the computer is equipped with an nVidia graphics card), network data transfer can be achieved by tunnelling INET sockets via ssh.

In the current version, FITS files are saved by the server component (i.e., image transfer to the client is performed solely for visual inspection purposes); therefore, it is important that the server is launched by the same user that the client will subsequently run.

3.3 System core

All utilities ensuring the operation of the system as a whole are hosted on an industrial-grade mini-PC running Calculate Linux. Upon switching on the computer, the following daemons are launched:

- detector control;
- providing network access to the serial port emulator for diagnostic purposes;
- stepper motor control and generation of FITS headers reflecting their current state;
- acquisition of current data from the control system of the telescope at which the observations are being conducted, with generation of the corresponding FITS headers.

By connecting to the computer via ssh or by proxying the required ports using ssh, the device can be controlled remotely. By writing scripts in bash or another interpreted programming language, routine operations can be automated (e.g., collecting frames for panorama generation or sequentially pointing the telescope at $100 \div 200$ areas that are uniformly distributed over the sky, and imaging stellar fields for updating the PCS).

4 First results

Figure 2 shows the first results obtained during observations at the BTA. Despite the poor image quality (full width at half maximum of about $2 \div 2.5''$) and the effective split of the image into speckles at short exposures, the centroid measurement accuracy was no worse than $0.1''$, which made it possible to construct plots of the telescope tube oscillations over 40 minutes of the accumulation of frames with exposures of 0.1 s. A peak in the $0.7 \div 0.8$ Hz range is clearly visible, which had been observed previously as well. These oscillations are a property of the telescope control system (feedback loops combined with the mechanics), since when pointing at Polaris with all control systems completely disabled (including the bearing oil supply), only aperiodic oscillations caused by wind and atmospheric density waves were observed.

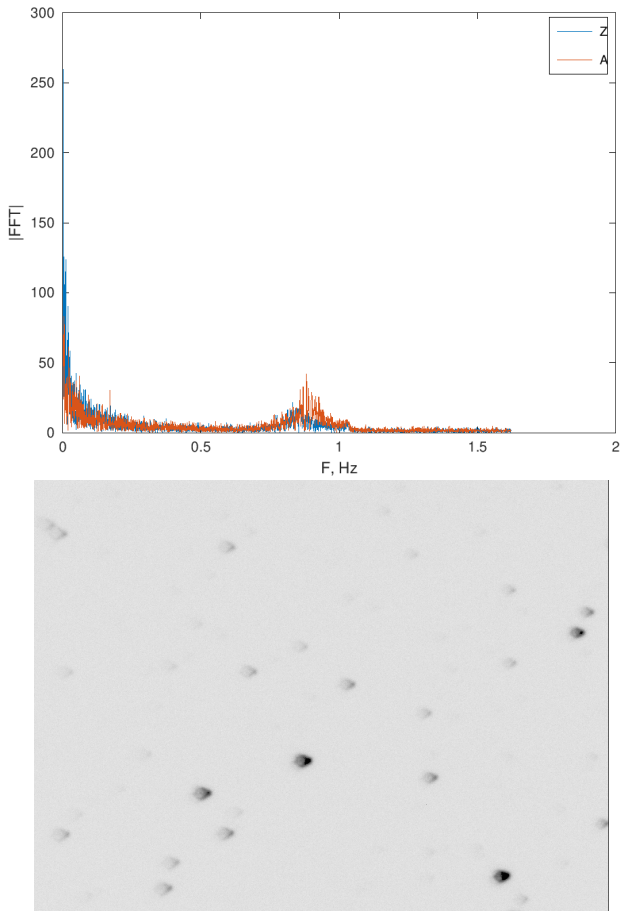

Fig. 2. Oscillation spectrum of the BTA in the object tracking mode (top); an example of coma at the edge of the field of view (bottom).

The bottom panel of Fig. 2 shows an example of coma at the edge of the image (the coma direction corresponds to motion along the telescope's Z axis). The coma is even more pronounced in the corner farthest from the center. Even a basic analysis of the files obtained in this manner using the SExtractor[4] utility (treating the coma as an ellipse whose semi-major axis is directed toward the aberration center) will allow the aberration axis of the PM to be aligned with the rotation center of the primary focus rotary table to an accuracy of no worse than 0.1 mm (one arcsecond at the BTA primary focus). The procedure for determining the position of the aberration center consists of computing the coordinates of the intersection point of the coma axes of stellar images at the edge of the field of view.

Testing of the device at the Zeiss-1000 telescope was not fully successful due to meteorological conditions: the

[4] https://sextractor.readthedocs.io/en/latest/Introduction.html

image quality was worse than $3''$. Furthermore, owing to recent modifications to the optical layout of the telescope, its field of view was significantly reduced. As a result, no image aberrations were detected across the entire field available for investigation. It is necessary to repeat the study using subarcsecond images (in this case aberration analysis may allow the most optimal value for carrying out the telescope focus from its flange to be determined). Construction of focusing curves yielded the following relationship between the instrumental coordinate z (mm) and the secondary mirror encoder reading (F, mm):

$$F = 15.72 + 8.926 \cdot 10^{-2} z \pm 0.01$$

or

$$F = 15.76 + 8.56 \cdot 10^{-2} z + 2.514 \cdot 10^{-5} z^2 \pm 0.005,$$

which allows the achievable range of carrying out the focus to be determined, which is slightly over two hundred millimeters.

5 Prospects

The first test run of the device demonstrated the need to supplement it with an additional node: an objective with an adjustable Foucault knife introduced into the light beam. A review of the literature led to the conclusion that the shadow method, once regarded as exclusively qualitative, can also be used quantitatively. This would allow the working surface shapes of telescope mirrors to be studied at a significantly higher resolution than that provided by the Shack – Hartmann method with a 40×40 microlens raster, or, all the more so, the classical Hartmann method. Unfortunately, the design of the device does not allow such a node to be permanently installed; to obtain foucaultgrams, it will need to be mounted manually; thus, remote observations in this case will not be possible.

A drawback of the TeA detector – its extremely small pixel size – can be turned into an advantage when working with the classical Hartmann method (a pre-focal mask mounted on the primary focus cabin shutters is used at the BTA; a mask mounted directly at the telescope tube entrance is used at Zeiss-1000). The high displacement speed along the device's z axis, together with the small displacement range required to obtain pre- and post-focal images, allows the accuracy of mirror surface exploration through this method to be improved (when the detector was displaced by the BTA focusing mechanism, the star had time to shift by several tenths of an arcsecond during the displacement, introducing significant errors into the method).